International Journal of
Molecular Sciences

MDPI

Article

Apoptosis Induction of *Agave lechuguilla* Torrey Extract on Human Lung Adenocarcinoma Cells (SK-LU-1)

Luis Alberto Anguiano-Sevilla [1], Eugenia Lugo-Cervantes [2], Cynthia Ordaz-Pichardo [3], Jorge Luis Rosas-Trigueros [4] and María Eugenia Jaramillo-Flores [1,*]

1 Escuela Nacional de Ciencias Biológicas, Instituto Politécnico Nacional IPN; Av. Wilfrido Massieu Esq. Cda. Manuel Stampa S/N Col. Unidad Profesional López Mateos, Alcaldía Gustavo A. Madero, Ciudad de México 07738 Mexico; luis.alberto.anguiano@gmail.com
2 Centro de Investigación y Asistencia en Tecnología y Diseño del Estado de Jalisco A. C., CIATEJ, Camino arenero 1227, Col. El Bajío del Arenal, Zapopan 45019, Mexico; elugo@ciatej.mx
3 Escuela Nacional de Medicina y Homeopatía, Instituto Politécnico Nacional IPN, Guillermo Massieu Helguera 239, Col. La Escalera, Alcaldía Gustavo A. Madero, Ciudad de México 07320, Mexico; cordaz@ipn.mx
4 Escuela Superior de Cómputo, Instituto Politécnico Nacional IPN, Juan de Dios Bátiz y Miguel Othón de Mendizábal S/N Col. Unidad Profesional López Mateos, Alcandía Gustavo A. Madero, Ciudad de México 07738, Mexico; jlrosas@ipn.mx
* Correspondence: jaramillo_flores@hotmail.com; Tel.: +52-55-5729-6000 (Ext. 57873)

Received: 12 October 2018; Accepted: 24 November 2018; Published: 27 November 2018

Abstract: In this study, an ethanol extract of *Agave lechuguilla* was evaluated against six carcinogenic cell lines (HCT-15, MCF-7, PC-3, U-251, SK-LU-1 and K-562) with an inhibition of 75.7 ± 2.3% against the SK-LU-1 line. Based on the previous result, the extract was hydrolyzed and fractionated, to which the IC_{50} was determined; the cell line was more sensitive to the fractionated extract with an IC_{50} 6.96 ± 0.15 µg/mL. Characterization by mass spectrometry showed the presence of kaempferol, quercetin and a flavonoid dimer formed by afzelechin-4β-8-quercetin, according to the generated fragmentation pattern. The fractionated extract presented cell death by apoptosis with 39.8% at 24 h. Molecular docking was performed with the molecules found to try to describe cell death by apoptosis through death receptors such as FasCD95, TNF-R1, DR4/5 and blocking signaling on the EGFR and K-Ras MAPK/ERK pathway, as well as through the intrinsic pathway activating tBID, which promotes the amplification of the apoptotic signal due to the activation of caspase-3, and consequently caspase-7. In addition to the activation of the IIb complex associated with cell death due to necroptosis.

Keywords: *Agave lechuguilla*; apoptosis; cytotoxic activity; molecular docking; mass spectrometry

1. Introduction

Cancer is one of the main health problems worldwide; the disease is characterized by abnormal cell growth and invasive behavior [1]. In 2018, lung cancer is the leading cause of death among different types of cancer, with 1,761,007 deaths reported for both sexes in all ages worldwide, representing 18.4% of deaths associated with cancer [2]. The cancer genome is incredibly complex, showing uncontrolled cell growth [3,4], and in particular lung cancer is highly invasive and prevalent disease that arises as a malignant tumor in the cells of the respiratory tract of the epithelium [5].

Histopathologically, it is classified into two groups: Small cell lung cancer (SCLC) and non-small cell lung cancer (NSCLC). Eighty-five percent of lung cancer cases are comprised of NSCLC, and this may include different subtypes of lung cancer such as: Adenocarcinoma, squamous cell carcinoma and large cell carcinoma [6]. The most common lung cancer is adenocarcinoma, which comprises about 40% of all lung cancers [7]. The SK-LU-1 adenocarcinoma cell line presents epithelial morphology and grows in adherent culture, is mutant K-Ras and does not exhibit telomerase activity. The K-Ras gene codes for a G-protein that participates in the EGFR cascade, whose mutations are found on chromosome 12, generating the substitution of an amino acid that determines the constitutive activation of the gene in the form of GTP, and consequently the continuous transmission of the RAF-MAP kinases cascade [7]. Most SCLCs acquire resistance to multiple drugs, whereas NSCLCs tend to be intrinsically resistant to chemotherapy [8]. The EGF receptor is expressed on the cell membrane and patients with lung adenocarcinoma can be classified as EGFR positive or EGFR negative, according to whether or not there is a mutation in the receptor [9]. The causes of lung cancer have been associated with family background with history of the disease [8], use of hormone therapy [9], tobacco smoke in the environment [10], air pollution (increase of 10 μg m^{-3} PM, increase of 10 ppb in SO_2, increase of 10 ppb in NO_2) [11], smoke from cooking oil [12], domestic combustion smoke (heating and cooking) [13], patient history (tuberculosis, emphysema, chronic bronchitis, parenchymal infection) [14] and high fruit consumption [15]. During the last decades, flavonoids have gained importance due to their antioxidant capacity and their effects against different types of cancer, reducing cellular viability, migration and invasion, and therefore, their possible therapeutic application [1,16]. *Agavaceae* belongs to the *Agave* genus, which has more than 400 species that grow in semi-arid and arid climates [17–20]. The *Agave lechuguilla* presents a wide range of secondary metabolites among which there are triterpenes, tannins, volatile coumarins, alkaloids, reducing sugars, steroidal saponins and flavonoids [17,21–24]. Therefore, the purpose of this work was to determine the cytotoxicity of an ethanolic extract of *Agave lechuguilla*, the hydrolyzate of the extract and the fraction enriched in flavonoids, against lung cells (SK-LU-1), to determine cell death by apoptosis and to elucidate the activation of cell death receptor signaling (extrinsic pathway) and mitochondria-dependent apoptosis (intrinsic pathway) by molecular docking, which also proved to activate molecular targets.

2. Results & Discussion

The ethanolic extract of *A. lechuguilla* (EE), has a content of phenols of 23.44 ± 1.47 μg Eq of gallic acid mg $extract^{-1}$, and an antioxidant activity of 1962.99 ± 211.86 μM Eq of Trolox mg $extract^{-1}$, while the hydrolysate (HE) and the enriched extract of *A. lechuguilla* have reduced polyphenols content of 37.45 ± 3.50 and 2.69 ± 0.12 μg Eq gallic acid mg $extract^{-1}$, respectively, Table 1.

Table 1. Concentrations of total polyphenols, total flavonoids and antioxidant capacity.

Extract of *A. lechuguilla*	Total Polyphenols [1]	Total Flavonoids [2]	TEAC [3]	ORAC [3]
Ethanolic	23.44 ± 1.47	19.62 ± 1.23	87.36 ± 3.57	1962.99 ± 211.86
Hydrolyzed	37.45 ± 3.57	3.08 ± 0.00	46.53 ± 0.72	1216.83 ± 4.88
Fraction	2.69 ± 0.12	1.47 ± 0.00	6.12 ± 0.91	49.20 ± 0.80

[1] μg Eq gallic acid mg $extract^{-1}$, [2] μg Eq quercetin mg $extract^{-1}$, [3] μM Eq Trolox mg $extract^{-1}$. Mean values ± SD of replicate samples analyzed in triplicate.

By means of UPLC-ESI (+)-MS analysis, the major metabolites were identified in the three different extracts shown in Table 2. The ethanolic extract of *A. lechuguilla* has seven components, five of which are saponins, whose glycones have four to five sugar units between hexoses and pentoses; two flavonoids identified as kaempferol and quercetin according to their fragmentation pattern [17,25,26].

In the hydrolyzed extract, 10 compounds were found, maintaining the signals of kaempferol and quercetin, and due to hydrolysis, the molecular weights 414, 416 and 430 were found, which correspond to different sapogenins found in the ethanolic extract. In addition, two isomers of a flavonoid dimer were found, which presented the same fragmentation pattern, associating the spectra that describe weights corresponding to afzelechin (flavan-3-ol), whose difference in weight between *m*/*z* 579.397 and 304.304 is 275.093 described by [Afzelechin + H] and quercetin (flavonol) with a weight of 302 g/mol reported as [Quercetin + 2H], which conforms to the junction in position (4β-8) since the flavan-3-ols are linked by C4 and the flavanols in C8.

The presence of this biflavonoid identified in the mass spectrum of the extract fraction, could be due to the fact that these compounds are found in very low concentrations that they could not be detected in the ethanolic extract or, during hydrolysis, there were ruptures of polymeric flavonoid units, and this lead to new constituents.

Moreover, five compounds were found in the fractionated extract of *A. lechuguilla*, two of them from the ethanolic extract: kaempferol and quercetin, and the isomers of the dimeric flavonoid.

Table 2. Ion assignation and formula condensed of metabolities in extracts from *A. lechuguilla*.

Possible Molecule	Rt [1]	*m/z*	Ions Assignation	CF [2]
Ethanolic extract of *A. lechuguilla*				
Tigogenin-glycoside or Neotigogenin-glycoside or Smilagenin-glycoside or Sarsasapogenin-glycoside	0.42	417.339	[M + H]	$C_{56}H_{92}O_{27}$
		579.396	[M + Hex + H]	
		741.450	[M + Hex + Hex + H]	
		903.506	[M + Hex + Hex + Hex + H]	
		1035.549	[M + Hex + Hex + Hex + Pent + H]	
		1197.605	[M + Hex + Hex + Hex + Pent + Hex + H]	
Hecogenin-glycoside or Sisalagenin-glycoside or Gloriogenin-glycoside or Yuccagenin-glycoside	0.56	431.336	[M + H]	$C_{56}H_{90}O_{28}$
		593.375	[M + Hex +H]	
		755.429	[M + Hex + Hex + H]	
		917.484	[M + Hex + Hex + Hex + H]	
		1049.528	[M + Hex + Hex + Hex + Pent + H]	
		1211.584	[M + Hex + Hex + Hex + Pent + Hex + H]	
Kaempferol	5.06	245.082	[M − C_2H_2O + H]	$C_{15}H_{10}O_6$
		269.085	[M − H_2O + H]	
		287.096	[M + H]	
Quercetin	5.44	257.082	[M − H_2O − CO +H]	$C_{15}H_{10}O_7$
		285.080	[M − H_2O + H]	
		303.091	[M + H]	
Diosgenin-glycoside or Yamogenin-glycoside	6.09	415.325	[M + H]	$C_{50}H_{80}O_{22}$
		577.381	[M + Hex + H]	
		709.424	[M + Hex + Pent + H]	
		871.479	[M + Hex + Pent + Hex + H]	
		1003.523	[M + Hex + Pent + Hex + Hex + H]	
Tigogenin-glycoside or Neotigogenin-glycoside or Smilagenin-glycoside or Sarsasapogenin-glycoside	6.34	417.342	[M + H]	$C_{56}H_{92}O_{27}$
		579.397	[M + Hex + H]	
		741.451	[M + Hex + Hex + H]	
		903.506	[M + Hex + Hex + Hex + H]	
		1065.561	[M + Hex + Hex + Hex + Hex + H]	
		1197.606	[M + Hex + Hex + Hex + Hex + Pent + H]	
Tigogenin-glycoside or Neotigogenin-glycoside or Smilagenin-glycoside or Sarsasapogenin-glycoside	6.57	417.341	[M + H]	$C_{50}H_{82}O_{22}$
		579.396	[M + Hex + H]	
		741.451	[M + Hex + Hex + H]	
		903.506	[M + Hex + Hex + Hex + H]	
		1035.550	[M + Hex + Hex + Hex + Pent + H]	

Table 2. *Cont.*

Possible Molecule	Rt [1]	*m/z*	Ions Assignation	CF [2]
Hydrolyzed extract of *A. lechuguilla*				
Unknow	0.54	701.503 475.332 340.264	ND	ND
Unknow	0.68	701.503 475.332	ND	ND
Kaempferol	4.97	245.082 269.085 287.096	[M − C_2H_2O + H] [M − H_2O + H] [M + H]	$C_{15}H_{10}O_6$
Quercetin	5.34	245.082 257.085 261.135 285.080 303.091	[M − $C_2H_2O_2$ + H] [M − H_2O − CO + H] [M − C_2H_2O + H][M − H_2O + H] [M + H]	$C_{15}H_{10}O_7$
Diosgenin or Yamogenin	5.36	415.155	[M + H] [M + Na + H]	$C_{27}H_{42}O_3$
Tigogenin or Neotigogenin or Smilagenin or Sarsasapogenin	6.92	417.342	[M + H]	$C_{27}H_{44}O_3$
Unknow	7.12	449.326	ND	ND
Biflavonoid (isomer)	8.37	230.251 245.083 261.135 304.304 579.397	[Quercetin − 2CO − H_2O + H] [Quercetin − $C_2H_2O_2$ + H] [Quercetin − C_2H_2O + H] [Quercetin + 2H] [Quercetin + Afzelequin + 3H]	$C_{30}H_{22}O_{12}$
Biflavonoid (isomer)	8.56	230.251 245.083 261.135 304.304 579.397	[Quercetin − 2CO − H_2O + H] [Quercetin − $C_2H_2O_2$ + H] [Quercetin − C_2H_2O + H] [Quercetin + 2H] [Quercetin + Afzelequin + 3H]	$C_{30}H_{22}O_{12}$
Hecogenin or Sisalagenin or Gloriogenin or Yuccagenin.	10.01	431.296 453.216	[M + H] [M + Na + H]	$C_{27}H_{42}O_4$
Extract fraction of *A. lechuguilla*				
Kaempferol	4.99	245.082 269.085 287.096	[M − C_2H_2O + H] [M − H_2O + H] [M + H]	$C_{15}H_{10}O_6$
Quercetin	5.33	257.085 285.080 303.091	[M − H_2O − CO + H] [M − H_2O + H] [M + H]	$C_{15}H_{10}O_7$
Unknow	6.48	269.086 365.111	ND	ND
Biflavonoid (isomer)	8.54	245.083 304.306 579.399 601.381	[Quercetin − $C_2H_2O_2$ + H] [Quercetin + 2H] [Quercetin + Afzelequin + 3H] [Quercetin + Afzelequin + Na + 3H]	$C_{30}H_{22}O_{12}$
Biflavonoid (isomer)	8.88	245.083 304.306 579.399 601.381	[Quercetin − $C_2H_2O_2$ + H] [Quercetin + 2H] [Quercetin + Afzelequin + 3H] [Quercetin + Afzelequin + Na + 3H]	$C_{30}H_{22}O_{12}$

[1] Retention time in minutes; [2] CF, condensed formula; Afzelequin: 274 *m/z*; Hex: $C_6H_{10}O_5$ Hexose 162 *m/z*; Pent: $C_5H_8O_4$ Pentose 132 *m/z*; ND, Not determined. Supplementary materials (Figure S1–S22) show the interpretation of the mass spectra.

The results of spectometry show the presence of kaempferol (Figure 1a), quercetin (Figure 1b) and the dimer of flavonoid (afzelechin 4β-8 quercetin) (Figure 1c).

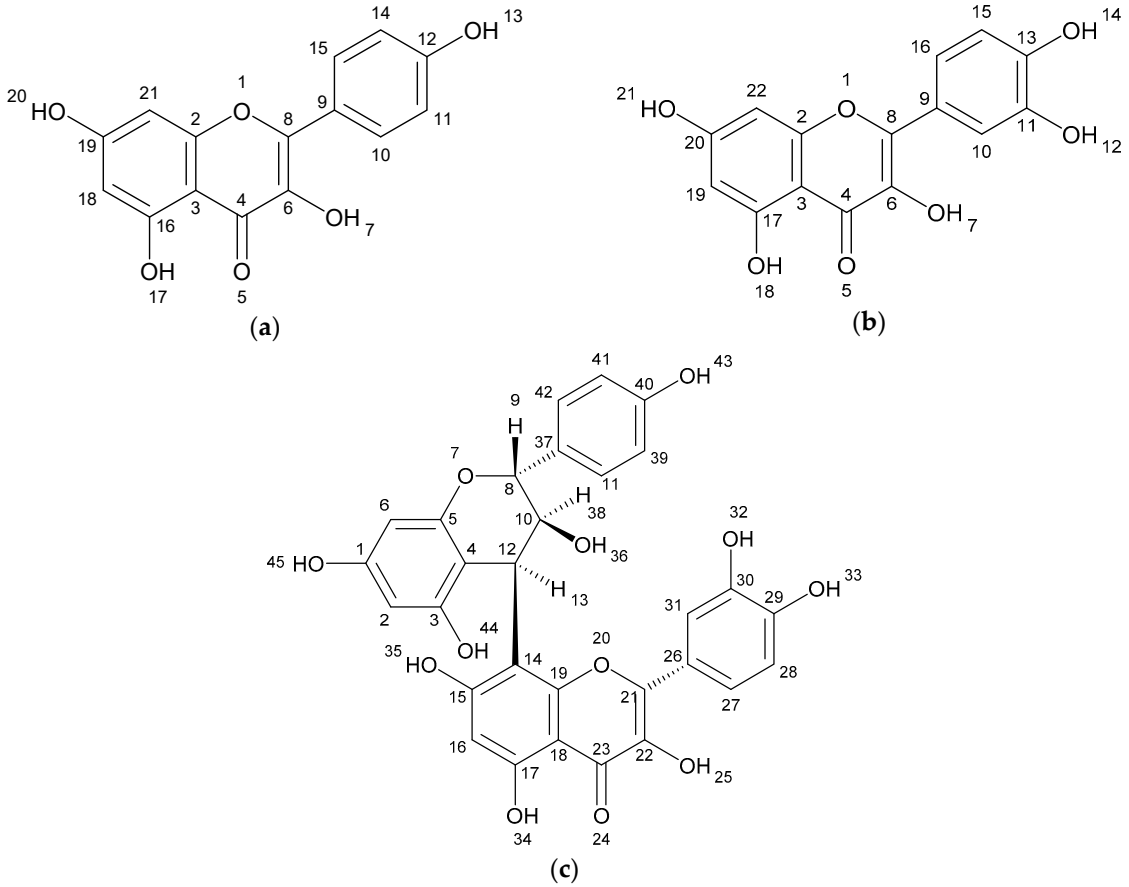

Figure 1. Structure of flavonoids and biflavonoid dimer with numbers associated to *in silico* results. (**a**) Kaempferol 287 g/mol (**b**) Quercetin 302 g/mol, and (**c**) Biflavonoid (afzelequin 4β-8 quercetin), 574 g/mol.

Primary screening on six cancer cell lines using ethanolic extract of *A. lechuguilla* at 50 µg/mL (Table 3), showed growth inhibition on the SK-LU-1 cell line in 75.7 ± 2.3% inhibition, followed by the HCT-15 line with 33.4 ± 3.6%, being the most sensitive to the extract, and compared to healthy cells, which were only inhibited in 1.2 ± 0.5%. The most sensitive line against the *A. lechuguilla* extract was SK-LU-1 (lung). Note that the two cell lines (HCT-15 and SK-LU-1) most sensitive to the extract fraction are K-Ras mutants.

Table 3. Percentage of cellular inhibition of ethanolic extract of *A. lechuguilla*.

Grow Inhibition [1] [%]						
Control	**HCT-15**	**MCF-7**	**PC-3**	**U-251**	**SK-LU-1**	**K-562**
1.2 ± 0.5	33.4 ± 3.6	10.5 ± 4.0	11.5 ± 1.8	24.0 ± 2.6	75.7 ± 2.3	17.1 ± 1.0

[1] Concentration of treatment of 50 µg *A. lechuguilla* extract/mL; Control, Cos-7 monkey kidney cells; Mean values ± SD of replicate samples analyzed in duplicate.

Due to the sensitivity of the SK-LU-1 line to the extract, the IC_{50} of the (a) ethanolic extract (EE), (b) hydrolyzed extract (HE) and the c) extract fraction (EF) of *A. lechuguilla* was determined on the SK-LU-1 cell line. The IC_{50} of the ethanolic extract (EE) was 109.40 ± 0.07 µg/mL, compared to the hydrolyzed extract (HE) of 133.9 ± 0.10 µg/mL, whose value increases due to the presence of free sugars, which probably work as a substrate for the SK-LU-1 cell line, so that the inhibitory power

is reduced. Moreover, it was found that for the extract fraction (EF) of *A. lechuguilla* the IC_{50} was 6.96 ± 0.15 µg/mL, the concentration required decreases at the same time by reducing the viability 15.7 times with respect to the ethanolic extract, due to the enrichment of active phenolic compounds, lower concentration of polar compounds and the elimination of free sugars. The results of IC_{50} at 24 and 48 hours of exposure, showed that the most promising treatment is better at higher dose in shorter period. Cytotoxicity data with the ethanolic extract of *A. lechuguilla* found an IC_{50} at 89.0, 128.0 and >150.0 µg/mL of extract against cell lines HeLa, Vero and MCF-7, respectively [27]. Furthermore, for quercetin on lung cells an IC_{50} of 34.15 ± 10.82 µg/mL has been reported [28], a concentration five times higher than the one found by the enriched extract of this study. The extract of the fraction of *A. lechuguilla* turned out to be the one with greater inhibitory effect, therefore, the induction of apoptosis was determined by the translocation assay of phosphatidylserine, demonstrating apoptosis induction. The results show an early apoptosis in the right lower quadrant of Figure 2 (Annexin $V^+/7\text{-}AAD^-$) with 3.56% at 6 h and 17.30% at 24 h, and a late apoptosis in the upper right quadrant (Annexin $V^+/7\text{-}AAD^+$) that goes from 5.96 to 6 h until reaching a value of 22.5% at 24 h. It was important to include positive and negative controls in this experiment to ensure that the cell population of SK-LU-1 was a true reflection of the events that were taking place after treatment with the fractionated extract of *A. lechuguilla*.

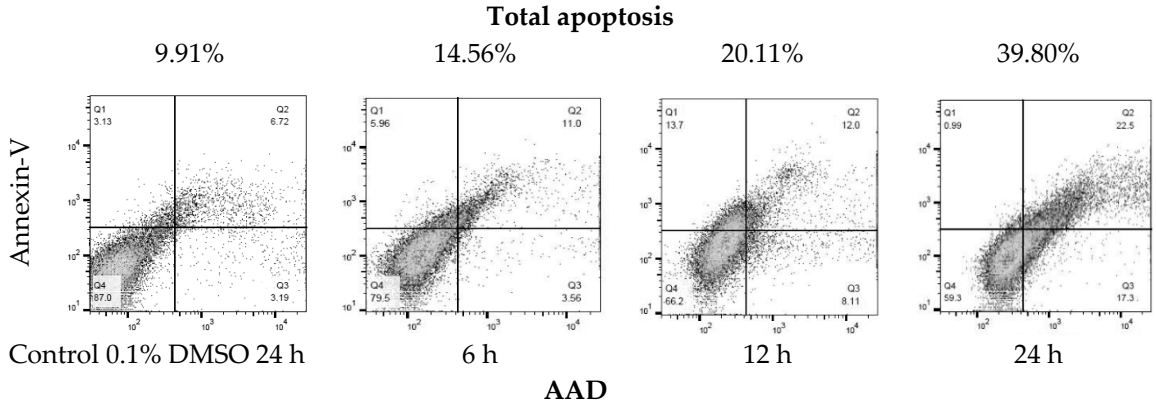

Figure 2. Translocation of phosphatidylserine by flow cytometry (Annexin V-FITC/7-AAD staining). Representative plots of SK-LU-1 cells cultured in the presence fractioned extract of *A. lechuguilla* with an IC_{50} = 6.96 µg/mL, are shown (total apoptosis-time of exposure).

Total apoptosis (programmed cell death) is the sum of early and late apoptosis, as reported in Table 4. At 6 h there is 14.56% of total apoptosis and 20.11% at 12 h, doubling the effect at 24 h with 39.80% total apoptosis. It is highlighted that cell death, due to necrosis, is lower at 24 h with 0.99%, it can be associated that the extract has a controlled death of these cells.

Table 4. Cells of SK-LU-1 response to treatment with fraction extract of *A. lechuguilla*.

Treatment [h]	Live Cells	Early Apoptotic Cells	Late Apoptotic Cells	Necrosis Cells	Total Apoptosis
			[%]		
Control	87.00	3.19	6.72	3.13	9.91
6	79.50	3.56	11.00	5.96	14.56
12	66.20	8.11	12.00	13.70	20.11
24	59.30	17.30	22.5	0.99	39.80

One strategy to improve our comprehension of apoptotic mechanisms, it was in silico studies, that look in space for the most favorable energetic conformation of a protein–ligand complex activating the signaling cascades or inhibiting the receptors as the case may be [29,30]. In T cells type I, cell death signaling by the extrinsic pathway is sufficient to carry out the apoptosis. In this case the SK-LU-1 lung cells are type II, which means that they require an amplification of apoptotic signaling

through the extrinsic and intrinsic pathways. The results of the interactions of the ligands and proteins by molecular docking are shown in Table 5; they determine the spontaneity of the reaction due to its negative free energy, hydrogen bonding, polar and hydrophobic interactions. The biflavonoid (afzelechin 4β-8 quercetin) activated the membrane receptor TNF-R1, forming hydrogen bonds with the T89 residue, polar interactions with S81, N92 and E135, as well as non-polar interactions with P90. By the extrinsic pathway, the bond with TNF-R1, activated procaspase-8 to form complex IIa (Caspase-8, FADD and RIP1), and thus, to activate Caspase-8 which in turn activates Caspase 3, and induces apoptosis, or the formation of the IIb complex (Caspase-8, FADD, RIP1, RIP3 and MLKL), thus, activating the necroptosis pathway. Moreover, the activation of DR4 is generated by the formation of hydrogen bonds with T129 and polar interactions with H270, in addition to non-polar interactions with C180 and V152. Experimental data indicate that the residues that activate this receptor (DR4) and its activation, send the signal to acetylate the adapter protein FADD, and to activate caspases 8 and 10, which at the same time activate caspase 3 to trigger apoptosis.

Also by the extrinsic pathway, the binding with the Fas/CD95 receptor acetylates to caspase 8 and 10, this ternary complex is commonly known as DISC composed of Fas, FADD and caspases-8 and -10 [31], which triggers activation of caspase 3, inducing apoptosis. By the intrinsic pathway of the mitochondria-dependent apoptosis, activation by the diflavonoid may be due to the fact that it is a stress promoter for the cell, which culminates in the mitochondrial outer membrane permeabilization (MOMP), allowing the release of proteins from the mitochondrial intermembrane space. This happens in T cells type II because the apoptotic signal needs to be amplified by caspases 3 and 7 [32,33]. In case the biflavonoid crosses the cell membrane, by active transport of K^+/Na^+ pumps or even by the calcium–sodium ion exchanger, it can activate the signaling cascade of the binding with the Fas/CD95 receptor by the direct interaction of the biflavonoid with tBID through the R71 and S78 residues; however, BID (BH3 interacting-domain death agonist)is directly activated by caspase 8, generating a tBID, moving to the mitochondria to release cytochrome C (prior stimulation of the Bax–Bak complex, members of the pro-apoptotic Bcl-2 family) [32], to immediately form the caspase-9 Apaf1 complex, which activates caspase-6 and caspase-3 to induce apoptosis. Quercetin interacts with TNF-R1 by hydrogen bonds with residues T89 and T147, by polar interactions with residues N92, N34, T147, P90 and V91, as well as by non-polar interactions, which can generate complexes IIa and IIb; the latter complex mostly has non-polar interactions with RIP1 in residues V75, V76, L78, M92 and L129. Polar interactions with MLKL and residues R210, Q236, E250, K331 and N336 can generate cell death due to necroptosis. At the same time, quercetin activates DR4 by hydrogen bonds with the T129 residue and by E155 by polar interaction, by the extrinsic pathway. By the intrinsic pathway, it could be activated only if it could cross the cell membrane since it only interacts with tBID through hydrogen bonds with R63, R71, and S78, that generate cytochrome C and the activation of caspase-3, and this can activate caspase-7.

Kaempferol is the only molecule that interacts with the Fas/CD95 receptor via a hydrogen bond with the W189 residue, this means that the extrinsic/intrinsic pathways can be equally activated, followed by the RIP complex with caspase-8, -10, activate BID; it becomes tBID through a translocation (that can be activated with interaction by a hydrogen bond with S78), and sends a signal to the BAX complex (polar interactions with D31, N31, S98, T151, S154, L203)-BAK that stimulates cytochrome C to form Apaf-1 with caspase-9 and to induce apoptosis by the activation of caspase-3 (shows hydrogen bonds interactions with H121, Q161, C163, R64, Q161 and A162, and polar interactions R64, E123, Y204 and R207).

Table 5. Summary of free energy, inhibition constant (K_i) and molecular interactions from metabolites determinate in fraction extract of *A. lechuguilla*.

Molecular Docking			Hydrogen Bonds		Polar Interactions		Hydrophobic Interactions	
Protein/Enzyme	**Free Energy [a]/K_i [b]**	**Ligand**	**Atom/aa**	**DST [c]**	**Atom/aa**	**DST [c]**	**Atom/aa**	**DST [c]**
Death Receptor Signaling								
Fas/CD95	+0.38/---	Docetaxel	---	---	---	---	---	---
	+0.13/---	Kaempferol	O1/W189	3.18	---	---	---	---
	+0.13/---	Quercetin	---	---	---	---	---	---
	+0.48/---	Biflavonoid	---	---	---	---	---	---
TNF-R1	−6.35/245.01	Docetaxel	O8/T89	3.11	O12/T89	3.71	---	---
			O11/T89	3.44	H4/T89	3.35	---	---
			---	---	O2/T89	3.84	---	---
			---	---	O9/T89	3.50	---	---
			---	---	---	---	---	---
			O6/T89	2.89	H3/T89	2.23	C14/P90	3.34
			O7/T89	3.01	H4/T89	2.05	C15/P90	3.52
			O5/T147	3.09	O4/N92	3.70	C8/V91	3.48
	+21.13/---	Kaempferol	---	---	O3/N92	3.81	---	---
	−5.03/206.98	Quercetin	---	---	H2/N34	3.76	---	---
			---	---	H2/T147	3.63	---	---
			O3/T89	2.81	O9/S81	3.37	C13/P90	3.75
			---	---	H18/S81	3.49	C30/P90	3.64
			---	---	H14/T89	2.04	C21/P90	3.61
			---	---	O9/N92	3.00	C24/P90	3.80
	−4.63/405.84	Biflavonoid	---	---	H18/N92	2.07	---	---
			---	---	H17/E135	1.99	---	---
			---	---	O7/E135	3.03	---	---
			---	---	H16/E135	2.13	---	---
			---	---	O8/E135	2.90	---	---
DR4	−4.29/712.86	Docetaxel	O6/R158	3.33	H4/T129	3.51	---	---
			---	---	O7/E155	2.90	---	---
			---	---	H3/E155	2.00	---	---
			---	---	O7/R158	3.49	---	---
			---	---	H3/R158	3.41	---	---
			---	---	O5/R158	3.80	---	---
			---	---	H2/R158	3.68	---	---
			---	---	H2/T149	3.67	---	---

			---	---	H15/T129	2.26	---	---
	−4.39/607.34	Kaempferol	---	---	O1/T129	3.75	C13/V152	3.26
			---	---	O1/E155	3.36	---	---
			---	---	O2/E155	3.31	---	---
			---	---	O4/E155	3.86	---	---
			---	---	O2/R158	3.31	---	---
			---	---	O5/H270	3.38	---	---
	−4.78/315.05	Quercetin	O1/T129	3.41	O1/E155	3.87	---	---
					O2/E155	3.64	---	---
					O4/E155	3.46	---	---
					O2/R158	3.17	---	---
	−5.12/176.35	Biflavonoid	O5/T129	3.02	H15/T129	2.26	C23/V152	3.35
			---	---	O5/H270	3.38	C24/V152	3.61
			---	---	---	---	C30/V152	3.39
			---	---	---	---	C13/C180	3.72
			---	---	---	---	C14/C180	3.29
	$-1.73/53.64 \times 10^3$	Docetaxel	O7/S22	3.15	---	---	---	---
	$-5.85/6.76 \times 10^3$	Kaempferol	O5/S22	3.17	O3/R39	3.55	---	---
			H2/S22	3.50	H1/R39	3.16	---	---
			H2/P23	3.72	O1/D40	3.08	---	---
DR5			---	---	O2/D40	3.77	---	---
			---	---	O4/D40	3.64	---	---
			---	---	H1/D40	3.85	---	---
	+6.28/---	Quercetin	---	---	---	---	---	---
	+204.31/---	Biflavonoid	---	---	---	---	---	---
Mitochondrial Control of Apoptosis								
	$-3.24/4.21 \times 10^3$	Docetaxel	O10/R84	2.57	---	---	---	---
	$-2.40/17.55 \times 10^3$	Kaempferol	O3/S78	2.19	---	---	---	---
	$-2.69/10.58 \times 10^3$	Quercetin	O6/R63	2.68	---	---	---	---
			O7/R63	1.95	---	---	---	---
tBID			O7/R71	1.76	---	---	---	---
			O6/R71	1.88	---	---	---	---
			O3/S78	1.88	---	---	---	---
			O11/R71	2.95	---	---	---	---
	$-2.77/9.29 \times 10^3$	Biflavonoid	O9/S78	2.17	---	---	---	---
	+0.02/---	Docetaxel	---	---	---	---	---	---
Bax	−5.33/122.89	Kaempferol	---	---	H1/D31	3.33	---	---
			---	---	O2/D31	3.36	---	---

			---	---	O4/D31	3.29	---	---
			---	---	O5/N31	3.70	---	---
			---	---	O5/S98	3.52	---	---
			---	---	H2/S98	3.65	---	---
			---	---	O2/T151	3.58	---	---
			---	---	O4/S154	3.57	---	---
			---	---	O4/L203	3.76	---	---
	+0.13/---	Quercetin	---	---	---	---	---	---
	+0.46/---	Biflavonoid	---	---	---	---	---	---
Bak	+0.14/---	Docetaxel	---	---	---	---	---	---
	+0.51/---	Kaempferol	---	---	---	---	---	---
	+0.13/---	Quercetin	---	---	---	---	---	---
	+0.42/---	Biflavonoid	---	---	---	---	---	---
Bcl-2	+0.04/---	Docetaxel	---	---	---	---	---	---
	+0.51/---	Kaempferol	---	---	---	---	---	---
	+0.13/---	Quercetin	---	---	---	---	---	---
	+0.42/---	Biflavonoid	---	---	---	---	---	---
Caspases								
Casp-3	−6.79/10.47	Docetaxel	O6/Y204	3.40	O4/T62	3.83	C26/H121	3.71
			O11/Y204	3.17	H1/T62	3.52	C43/C163	3.17
			---	---	O12/H121	3.53	C35/C163	3.25
			---	---	N1/H121	3.71	C29/C163	3.83
			---	---	H5/H121	2.90	C33/C163	3.41
			---	---	O8/Y204	3.07	C38/C163	3.75
			---	---	O2/Y204	3.57	C8/F256	3.76
			---	---	---	---	C4/F256	3.76
			---	---	---	---	C23/F256	3.25
			---	---	---	---	C21/F256	3.58
	−6.15/30.95	Kaempferol	O1/H121	3.12	O5/R64	3.38	C1/C163	3.45
			O5/Q161	3.09	O6/E123	2.76	C2/C163	3.35
			O1/C163	3.44	H3/E123	1.82	C3/C163	3.76
			H2/R64	3.80	O4/Y204	3.26	C4/C163	3.66
			H2/Q161	3.73	H1/Y204	3.59	---	---
			H2/A162	3.57	O3/R207	3.62	---	---
	+0.13/---	Quercetin	---	---	---	---	---	---
	+0.43/---	Biflavonoid	---	---	---	---	---	---
Casp-8	−1.94/38.07 × 10^3	Docetaxel	---	---	---	---	C39/K224	3.55
	−1.05/170.68 × 10^3	Kaempferol	---	---	O1/L224	3.20	---	---

	−1.13/147.65 × 10^3	Quercetin	---	---	---	---	C7/K224	3.68
			---	---	---	---	C11/K224	3.56
			---	---	---	---	O3/K224	3.75
			---	---	---	---	C1/K224	3.67
			---	---	---	---	C6/L224	3.75
	−0.41/502.84	Biflavonoid	---	---	---	---	C27/K224	3.53
			---	---	---	---	O8/K224	3.88
Necroptosis								
RIP1	ND	Docetaxel	ND	ND	ND	ND	ND	ND
	−7.66/2.44	Kaempferol	---	---	O5/N68	3.68	C10/L70	3.42
			---	---	H2/R71	3.65	C8/L78	3.38
			---	---	---	---	C11/L78	3.34
			---	---	---	---	C13/L78	3.62
			---	---	---	---	C13/L90	3.41
			---	---	---	---	C15/L90	3.65
			---	---	---	---	C11/M92	3.48
			---	---	---	---	C13/M92	3.03
			---	---	---	---	C15/M92	3.11
			---	---	---	---	C14/M92	3.32
	−7.64/2.53	Quercetin	---	---	O5/H136	3.72	C7/V75	3.66
			---	---	H2/H136	2.91	C11/V75	3.55
			---	---	---	---	C2/V76	3.66
			---	---	---	---	C3/V76	3.59
			---	---	---	---	C14/L78	3.89
			---	---	---	---	C14/M92	3.41
			---	---	---	---	C12M92	3.87
			---	---	---	---	C15/M92	3.88
			---	---	---	---	C11/L129	3.44
	+63.84/---	Biflavonoid	---	---	---	---	---	---
MLKL	ND	Docetaxel	ND	ND	ND	ND	ND	ND
	−4.98/225.37	Kaempferol	---	---	O3/R210	3.46	C10/L338	3.59
			---	---	H1/R210	3.85	C9/A348	3.56
			---	---	O1/K230	3.39	C10/A348	3.65
			---	---	H2/K230	3.77	---	---
			---	---	O5/E250	3.06	---	---
			---	---	H2/E250	2.09	---	---
			---	---	O2/S335	3.85	---	---
			---	---	O1/N336	3.59	---	---

			---	---	O2/N336	3.67	---	---
			---	---	H3/E351	2.16	---	---
	−5.28/135.30	Quercetin	O1/L230	3.00	O3/R210	3.81	C11/L338	3.66
			---	---	O7/Q236	3.38	C9/A348	3.42
			---	---	H4/Q236	3.74	C11/A348	3.46
			---	---	O5/E250	3.00	---	---
			---	---	H2/E250	2.06	---	---
			---	---	O6/K331	3.21	---	---
			---	---	H3/L331	3.30	---	---
			---	---	O1/N336	3.88	---	---
			---	---	O2/N336	3.79	---	---
			---	---	O4/N336	3.42	---	--
	+0.58/---	Biflavonoid	---	---	---	---	---	---
	ND	Docetaxel	ND	ND	ND	ND	ND	ND
FADD	+0.51/---	Kaempferol	---	---	---	---	---	---
	+0.13/---	Quercetin	---	---	---	---	---	---
	+0.45/---	Biflavonoid	---	---	---	---	---	---
Epidermal Growth Factor Receptor (MAPK/ERK Pathway), Transforming Growth Factor B Receptor & Multidrug Resistance Protein 1								
	ND	Docetaxel	ND	ND	ND	ND	ND	ND
	−6.16/30.34	Kaempferol	O2/S262	3.20	H2/H280	3.16	C8/P242	3.11
			O4/S262	2.88	O6/D238	3.07	C15/L245	3.51
			---	---	H3/D238	2.27	C14/L245	3.01
			---	---	O3/H280	3.61	C12/L245	3.28
			---	---	O4/S282	3.77	C9/P242	3.40
			---	---	---	---	C10/P242	3.34
EGFR	−6.82/10.10	Quercetin	O2/S262	2.96	O5/H280	3.87	C8/P242	3.08
			O4/S262	2.82	H2/H280	3.05	C13/L245	3.10
			---	---	O6/D238	2.85	C15/L245	3.39
			---	---	H3/D238	1.89	C14/L245	3.80
			---	---	H4/D238	3.72	C10/L245	3.51
			---	---	---	---	C11/P242	3.20
			---	---	---	---	C9/P242	3.55
	+7.77/---	Biflavonoid	---	---	---	---	---	---
	ND	Docetaxel	ND	ND	ND	ND	ND	ND
TGFβ receptor	+0.51/---	Kaempferol	---	---	---	---	---	---
	+0.13/---	Quercetin	---	---	---	---	---	---
	+0.44/---	Biflavonoid	---	---	---	---	---	---
K-Ras	ND	Docetaxel	ND	ND	ND	ND	ND	ND

	−6.72/11.93	Kaempferol	---	---	O6/S17	3.41	C11/A18	3.32
			---	---	H3/S17	2.50	---	---
			---	---	H1/D30	3.88	---	---
			---	---	H3/T35	3.89	---	---
			---	---	O5/D119	3.10	---	---
			---	---	H2/D119	2.18	---	---
			---	---	O5/S145	3.66	---	---
			---	---	H2/S145	3.14	---	---
	−7.45/3.45	Quercetin	O5/S145	3.43	O7/S17	3.63	C4/A18	3.88
			H2/D119	3.07	H4/S17	3.47	---	---
			H2/S145	3.60	O5/D119	2.92	---	---
			H2/K147	3.81	---	---	---	---
	−6.59/14.71	Biflavonoid	O12/K117	3.36	H18/S17	3.57	C9/Y32	3.81
			H21/L120	3.86	O6/D30	3.46	---	---
			---	---	H16/D30	3.83	---	---
			---	---	H15/D119	2.00	---	---
			---	---	O5/D119	2.76	---	---
			---	---	O4/K147	3.55	---	---
			---	---	O5/K147	3.54	---	---
ALK	ND	Docetaxel	ND	ND	ND	ND	ND	ND
	−3.01/6.25 × 10^3	Kaempferol	---	---	O5/E1167	3.53	C3/L1256	3.74
			---	---	H2/E1167	3.74	C5/L1256	3.37
			---	---	O6/D1203	3.01	O6/L1256	3.46
			---	---	H3/D1203	2.19	C11/L1256	3.17
			---	---	H2/D1270	2.74	C13/L1256	3.44
			---	---	O5/D1270	2.71	---	---
	−2.77/9.29 × 10^3	Quercetin	---	---	O7/N1254	3.54	C1/L1256	3.31
			---	---	H4/N1254	3.13	C2/L1256	3.42
			---	---	O6/D1270	3.13	C6/L1256	3.53
			---	---	H3/D1270	2.48	C7/L1256	3.59
			---	---	O7/D1270	3.72	C8/L1256	3.42
	+180.68/---	Biflavonoid	---	---	---	---	---	---
MEK	ND	Docetaxel	ND	ND	ND	ND	ND	ND
	+0.51/---	Kaempferol	---	---	---	---	---	---
	+0.14/---	Quercetin	---	---	----	---	---	---
	+0.90/---	Biflavonoid	---	---	---	---	---	---
MAPK	ND	Docetaxel	ND	ND	ND	ND	ND	ND
	−3.34/3.58 × 10^3	Kaempferol	O4/S51	3.03	O3/N49	3.47	C12/L53	3.54

			---	---	H1/N49	3.57	---	---
			---	---	O2/S51	3.67	---	---
			---	---	O3/S51	3.76	---	---
			---	---	H1/S51	3.88	---	---
			---	---	H3/R56	3.12	---	---
	−3.43/3.08 × 10^3	Quercetin	O7/S51	3.32	O2/S51	3.78	---	---
			H4/N49	3.55	H1/R56	3.13	---	---
			H4/S51	2.93	O7/N49	2.91	---	---
	−2.64/11.70 × 10^3	Biflavonoid	O12/S51	3.22	O3/N49	3.90	C22/V35	3.81
			H21/S51	3.31	H14/N49	3.54	C23/V35	3.80
			---	---	---	---	C19/P33	3.89
MRP1	ND	Docetaxel	ND	ND	ND	ND	ND	ND
	+0.50/---	Kaempferol	---	---	---	---	---	---
	+0.13/---	Quercetin	---	---	---	---	---	---
	+0.41/---	Biflavonoid	---	---	---	---	---	---

[a] Kcal/mol; [b] μM; [c] Distance [Å]; ND: Not determined; ---: No result generated; Å: angstroms; Atom: C—carbon; H—hydrogen, O—oxygen; aa—amino acids; amino acid nomenclature: C—cysteine, H—histidine, I—isoleucine, M—methionine, S—serine, V—valine, A—alanine, G—glycine, L—leucine, P—proline, T—threonine, F—phenylalanine, R—arginine, Y—tyrosine, W—tryptophan, D—aspartic acid, N—asparagine, E—glutamic acid, Q—glutamine, and K—lysine.

In silico studies with ginsenosides (steroids, glycosides and triterpenoid saponins) have shown the activation of Bax with threonine and asparagine residues [34], as in this study. In addition to the DR4 receptors, mostly with polar interactions with T129, E155, R158 and H27, and DR5 R39 and D40. In spite of not activating the TNF-R1 receptor, the action of kaempferol with the complex IIb that generates death by necroptosis was simulated. For this complex, the mechanism where RIP1 and RIP3 present nucleation has been proposed, a model in which the activation of RIP1 and RIP3 kinase and the RIP1/RIP3 amyloid scaffold reinforce each other. The amyloid scaffold can function as a crucial platform to recruit other components, such as MLKL (Mixed Lineage Kinase domain-Like protein), and to trigger the execution mechanisms of necroptosis [35]. RIP1 mostly present non-polar interactions (phosphorylations) with L70, L78, L90 and M92, which add up to necroptosis signaling; MLKL mainly presents polar interactions with residues R210, K230, E250, S335, N336 and E351. From phosphorylated RIP3, the activation of MLKL to phosphorylated MLKL, specifically in the residues of threonine and serine domain in their N-terminus, is necessary, but not sufficient to carry out necroptosis [31,35]. Docetaxel was the ligand as positive control, demonstrating the activation of the signaling cascade in the receptors of the cell membrane of TNF-R1 and DR4/5. Hydrogen bonds were generated in each receptor with T89 for TNF-R1, and R158 and S22 for DR4/5, which activate TRADD acetylases (TNF-R1) that directly stimulate caspase 8 and FADD (DR4/5), to the complex caspases 8 and 10, which at the same time stimulate caspase-3 that triggers cellular apoptosis, all of this via the extrinsic pathway.

Several genetic alterations have been described in NSLC, with EGFR, K-Ras and ALK being the most frequently altered oncogenes, which act as genomic drivers of tumors [36]. EGFR acts as a promoter in cell growth, proliferation and mortality. Kaempferol and the quercetin potently inhibit the intracellular phosphorylation of EGFR, due to its free energy that oscillates between −6.16 to −6.82 Kcal/mol, with polar interactions with D238 and exclusively hydrogen bridges with S262. The complex formed by these flavonoids activates the cytoplasmic domain of the tyrosine kinase receptor. Ras activates Raf kinase, by phosphorylation, and it should be mentioned that Ras mutated to K-Ras in this type of cancer is characterized by the fact that it leads to uncontrolled growth of the cell. However, the results of the molecular docking of K-Ras show a strong interaction of kaempferol, quercetin and the biflavonoid, which together inhibit this proliferation. K-Ras works as a switch (on/off) in signaling. When Ras works normally, it controls cell proliferation, but when it is mutated, control is interrupted and can proliferate continuously. By inhibiting the K-Ras kinase, K-Ras cannot phosphorylate MEK (MEK1 and MEK2), and through molecular docking, it was shown that there is no interaction between MEK and the flavonoids complex, which is favorable to stop the signaling pathway. Molecular docking showed that MAPK activation, despite not being desired, occurs at very high concentrations, 1000 times that of the flavonoids complex (3.08–11.70 $\times$ 10^3 μM) compared to inhibition concentrations against EGFR or K-Ras. That is, the concentration of the flavonoids should be very high to function as promoters in MAPK. By inhibiting this pathway, cell non-proliferation is associated, and since kaempferol, quercetin and biflavonoid activate death receptors by extrinsic and intrinsic pathways associated with apoptosis, cell proliferation decreases.

TGF-β participates both as an activator or suppressor of cell proliferation, suppressing tumors in normal cells, but promoting them in malignant cells [37], while MRP1 acts as a chemoprotector at the cellular interface and in the systemic circulation of multiple tissues [37,38], whose role contributes to drug sensitivity. In both cases by molecular docking, there were no interactions with the flavonoids.

The bioflavonoid (afzelechin 4β-8 quercetin) binds to the receptor TNF-R1 (Figure 3a) and DR4 (Figure 3b), and quercetin binds to TNF-R1 (Figure 3e) and DR4 (Figure 3f), activating death cell signaling by apoptosis; previously explained. Biflavonoid and the quercetin, activate the same death receptors, present the same type of interactions by hydrogen bonds with T89, polar interactions with N92 and non-polar interactions with P90, for TNF-R1; while for the DR4 receptor they only generate similar hydrogen bonds with T129. This may be due to the fact that the flavonoid contains a unit of quercetin in its molecule, part of these interactions are the same as those presented for quercetin in the form of a monomer. The interaction shown by kaempferol, quercetin and the dimer of flavonoid

with tBID, demonstrates the ability to amplify the apoptotic signaling, while kaempferol binds to DR5 (Figure 3d) and Fas/CD95 (Figure 3c) which has the peculiarity of activating the intrinsic pathway, and the kaempferol interaction with caspase-3 that helps the same amplification of the apoptosis.

The proteins of the Bcl-2 family can be classified into anti-apoptotic and pro-apoptotic, since there is a fine balance between both by homeostasis, if there is an overexpression of the anti-apoptotic proteins of the BCL-2 family, it prevents the release of cytochrome C from the mitochondria [34], given the results of simulation, no interactions with Bcl-2 were found; however, kaemperol with the Bax protein, instead of Bak, stimulates the apoptotic signaling cascade. Several studies have shown the activations against specific molecular targets, however, they have not studied the activations of other proteins that amplify the signaling of apoptosis by molecular modeling. In contrast, this study showed that the extract obtained can function as an activator of death receptors, as well as acting as an activator of molecular targets that amplify apoptosis signaling, such as caspase-8 and Bcl-2, in NSCLC [39,40].

On the other hand, there are receptors where inhibition is sought, as was the case of EGFR (Figure 3g) and K-Ras (Figure 3h), where having high affinity of the ligand for the active site of the receptor (EFGR) and of the protein (K-Ras), thus blocking the signaling cascade that promotes the proliferation of lung cancer cells SK-LU-1.

In addition to the participation of flavonoids in the aforementioned signaling pathways, these also participate in improving the immune response, which may contribute to ameliorate the health status. It is important to consider that even though chemotherapy continues to be the best treatment for cancer, resistance to drugs results in the reduction of intracellular levels of drugs at concentrations lower than therapeutic levels, resulting in poor chemotherapy. This resistance to drugs is increasing, so part of the solution is the search for compounds that selectively kill multidrug resistant cells (MDR), but not the parental cells from which they are derived (non-resistant), a phenomenon called collateral sensitivity (CS). CS is a type of synthetic lethality, wherein the genetic alterations accrued while developing resistance to one agent is accompanied by the development of hypersensitivity towards a second agent [41]. One of the four postulated mechanisms for this collateral sensitivity is the modulation of reactive oxygen species, where antioxidant compounds, such as flavonoids, become relevant. Given the accumulated evidence of the anticancer effects of flavonoids, coupled with little or no damage to normal cells, such as natural antioxidant quercetin whose LD50 is 160 mg/kg body weight, placing it as a potential therapeutic agent for be used in complementary therapy, however, there is also contradictory evidence, since on the one hand it is recognized as an anticancer agent, antiproliferative, chemopreventive, anti-inflammatory, even at the level of clinical trials, but on the other hand it is reported that 2-year studies quercetin showed carcinogenic activity in the kidney of the male rat, at a dose of 40–1900 mg/Kg/day. It is also well known that phenolic compounds at high doses can behave as pro-oxidants and present undesirable effects [42,43].

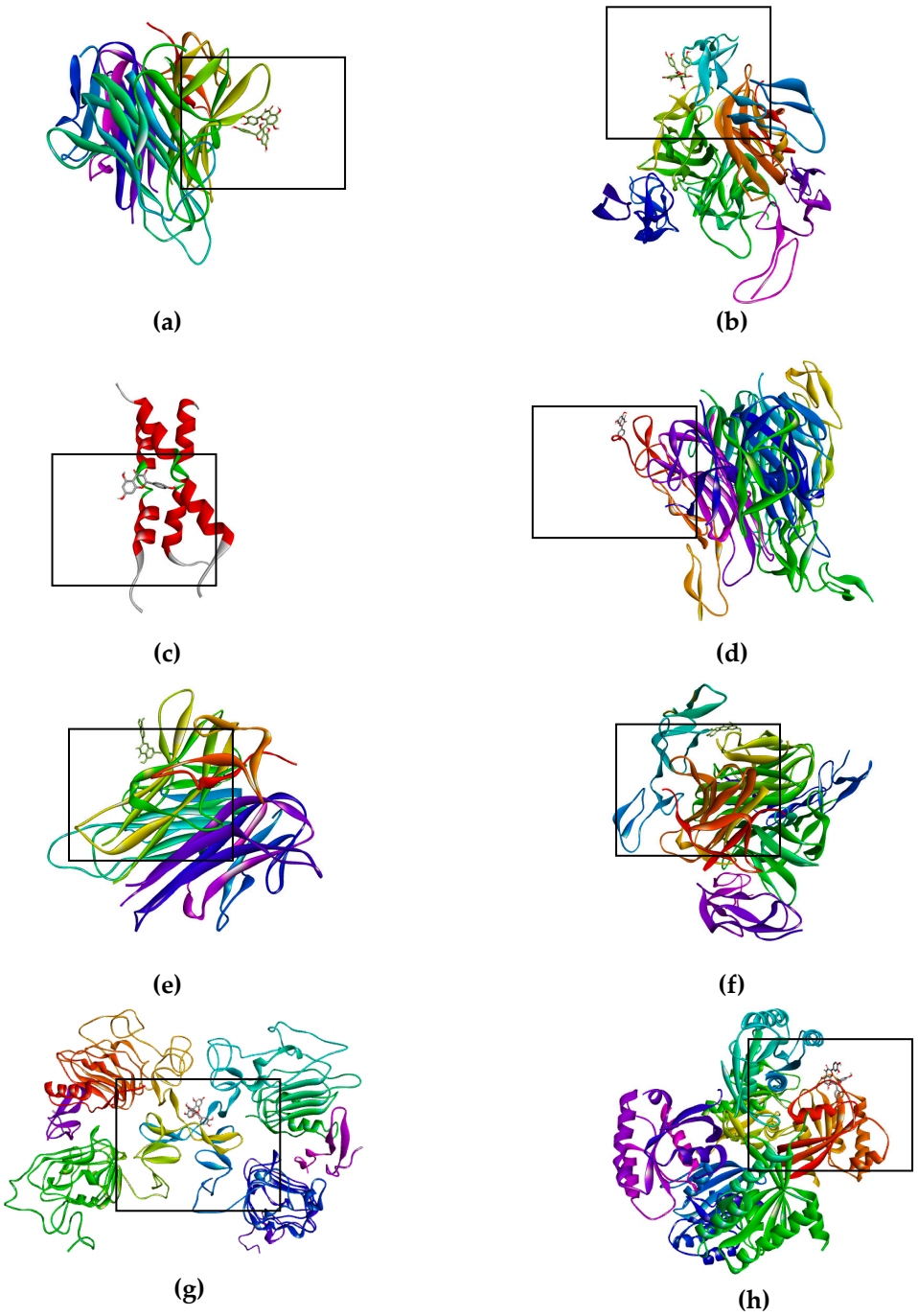

Figure 3. Binds of biflavonoid, kaempferol and quercetin with death receptor. The box indicates the binding region. (**a**) Biflavonoid binds to TNF-R1, (**b**) Biflavonoid binds to DR4, (**c**) Kaempferol binds to Fas/CD95, (**d**) Kaempferol binds to DR5 (**e**) Quercetin binds to TNF-R1, (**f**) Quercetin binds to DR4, (**g**) Biflavonoid binds to EGFR, and (**h**) Biflavonoid binds to K-Ras.

3. Materials and Methods

3.1. Plant Material

The *A. lechuguilla* was collected in San Bartolo (23°09′34.0″ N 100°34′10.7″ W) municipality of Villa De Guadalupe, San Luis Potosí State, Mexico in August 2017. The ripe leaves (25–50 cm) were air-dried (40 °C) and powdered (100 mesh).

3.1.1. Ethanolic Extract from *A. lechuguilla*

The dried powder of *A. lechuguilla* was extracted by sonication for 90 min with 96% ethanol (1:10 *w*/*v*). All the solvent was evaporated to dryness under reduced pressure (40 °C) (Ethanolic extract).

3.1.2. Hydrolysis Extract and Its Fractionated Hydrolyzed Extract of *A. lechuguilla*

Five milliliters of 50% aqueous methanol containing 1.2 M HCl and 0.04% (*w*/*v*) ascorbic acid as antioxidant were added to 50 mg of ethanolic extract dried sample. The hydrolysis was performed at 80 °C under reflux for 2 h and the extract was allowed to cool; the extract was subsequently diluted to 10 mL with methanol [44]. For subsequent analyzes 7 mL were evaporated to dryness under reduced pressure (40 °C) (Hydrolyzed extract of *lechuguilla*).To enrich the extract for phenolic compounds, 3 mL of hydrolysis extract of *A. lechuguilla* were eluted through a C18 cartridge (Sep-Pak classic, Part No: WAT051910, Water Co.), previous solvation with 3 mL H_2O (3×); then the cartridge was eluted again with 3 mL H_2O (3×) and the final 3 mL EtOH (3×) (Fraction extract of *A. lechuguilla*). All the solvent was evaporated to dryness under reduced pressure (40 °C).

3.2. Polyphenol and Flavonoid Total Quantification

The content of total phenolic compounds was determined by the Folin–Ciocalteau method [45] and the total of flavonoids compounds was quantified by the aluminum trichloride method [46].

3.3. Antioxidant Capacity Assays

The antioxidant capacity was determined by TEAC [47] and ORAC [48].

3.4. Mass Spectrometry

The samples were filtered (0.22 µm) with an injection volume of 3 µL, by using a BEH C18 1.7 µm column (Acquity UPLC, Waters) at 30 °C, with a flow of 0.3 mL/min with the following program: Solvent A (ACN) and solvent B (Water pH 2.5 TFA) 15% A 0 min, 35% A at 6.97 min, 35% at 15 min. The sample separated by the column was nebulized by ESI-Q-ToF (Xevo G2-XS QTof, Waters, Milford, MA, USA) and the ions that were collected in the range of 100 to 1300 Da, in positive (+) mode with the MassLynx software (v4.1, Waters, Milford, MA, USA) and the data were analyzed in the MestReNova software (v12.0.20910, Mestrelab Research S.L., http://mestrelab.com/)

3.5. Screening Cells Viability Assay by Sulforhodamine B

The cell viability determination of the ethanolic extract of *A. lechuguilla* (50.0 µg/mL) against six different cell lines was carried out: K-562 (chronic myeloblastic leukemia), HCT-15 (colon), MCF-7 (breast), PC-3 (prostate), U-251 (central nervous system) and SK-LU-1 (lung), with doubling times of 19.0 h, 18.1 h, 25.6 h, 28.7 h, 25.4 h and 25.4 h, based on this, the cell density was calculated 5000, 10,000, 5000, 7500, 7500 and 7500 cells/well, respectively; additionally, the cell line Cos-7 (monkey kidney) was used as control. The cell lines were provided by the Biological Testing Laboratory of the Chemistry Institute (Laboratorio de Pruebas Biológicas del Instituto de Química, UNAM, Mexico City, Mexico). The cells grew in RPMI-1640 culture medium supplemented with 10% FBS and with a mixture of 10.0% antibiotics-antimycotics and 2 mM glutamine. With the exception of line K-562, the remaining cell lines adhere to the culture bottles, to harvest them 1 mL Trypsin-EDTA (0.05%) is added, then the cells are detached from the plastic substrate by adding between 5–10 mL of culture medium to inactivate the trypsin. The cell suspension is centrifuged for 3 min (2000 RPM). Once the cellular package is formed, the culture medium is added to suspend them. Thirty microliters of inoculum are taken and mixed with 30 µL of trypan blue. The inoculum corresponds to 100 µL/well at the density described above. Each microplate was inoculated with two cell lines in triplicate, and incubated for 24 h at 37 °C, in an atmosphere of 5% CO_2 and 95% relative humidity. The ethanolic extract of the *A. lechuguilla* was dissolved in DMSO (Sigma-Aldrich, St Louis, MO, USA), to form a stock solution stored at −20 °C.

The stock solution was dissolved in culture medium to obtain 0.1% DMSO, then it was sterilized by filtration prior treatment and 100 µL were added, with a final volume of 200 µL/well. The microplate is incubated for 48 h under the same conditions previously mentioned. At the end of the incubation of the extract, the cell lines were fixed in situ by adding 50 µL of cold TCA 50.0%, incubated at 4 °C for 60 min, the supernatant was discarded, and the plates were washed five times with deionized water and dried at room temperature. The staining of the fixed cells was performed with a 0.4% SRB solution and incubated for 30 min at room temperature. The unbonded FBS was washed three times with 1.0% acetic acid and dried at room temperature. 100 µL of Tris buffer were added to the stained microplates and shaken for 10 min. The optical density was measured at λ-515 nm to the stained microplates [49]. Optical densities were averaged for the wells treated with the compound (ODt), the wells treated with DMSO (ODc) and the control wells, i.e. those that do not have cells, but have a compound (ODb). The IC was calculated with the following formula [50]:

$$\% \text{ IC} = 100 - (\text{ODt} - \text{ODb})/(\text{ODc} - \text{ODb}) \times 10 \quad (1)$$

3.6. Viability Assay by 3-(4,5-DiMethyl-2-Thiazolyl)-2,5-Diphenyl-2H-Tetrazolium Bromide

The cell viability through MTT formazan (Sigma-Aldrich, MO, USA) by the mitochondrial succinate dehydrogenase is present only in living cells. The absorbance value of formazan is directly proportional to the number of viable cells [51]. The fraction of *A. lechuguilla* extract was dissolved in DMSO (Sigma-Aldrich, MO, USA), to form a stock solution that was stored at −20 °C. The stock solution was dissolved in RPMI-1640 culture medium supplemented with 10% FBS and 1% antibiotic-antimycotic to obtain 0.1% DMSO, then it was sterilized by filtration prior treatment [52], they were exposed with the extracts at 24 and 48 h, with extract concentrations of 0.3 up to 300 µg/mL, DMSO was used as negative control (0.1%), and as positive control (5.0 µg/mL) (Paclitaxel from *Taxus brevifolia*, Sigma, Cat. No. T7402). The 96-well microplates were incubated with 8000 cells/well at 37 °C, 5% CO_2 and 95% relative humidity for 24 and 48 h. At the end of the treatment, they were removed and washed with PBS 1× twice to remove any residue, and 100 µL of MTT were added (1× = 5 mg/mL dissolved in medium without serum) per well and incubated for 4 h at 37 °C to allow the metabolism and formation of formazan crystals in darkness. At the end of this period, the supernatant of each well was removed and 100 µL of DMSO were added to allow solubilization of the formazan. The assays were performed in three independent replicates by triplicate. With the absorbance values obtained, the percentage of cell viability was calculated with the following formula:

$$\% \text{ Viability} = (\text{ODtreatment cells}/\text{ODcontrol cells}) \times 100 \quad (2)$$

The IC_{50} was calculated by means of a nonlinear regression analysis (percentage of viability vs. concentration Log) with the GraphPad Prism software (v7.00 GrapPad Software Inc., La Jolla, CA, USA).

3.7. Phosphatidylserine Translocation (Annexin V-APC)

We used the Apoptosis Detection Kit (Annexin V-APC Apoptosis Detection Kit BD Pharmigen), and the procedure was performed according to the manufacturer's protocol. SK-LU-1 cells were seeded in RPMI-1640 medium supplemented with 10% FBS and 1% antibiotic-antimycotic solution. When obtaining sufficient confluency of cells, these were seeded in 6-well plates at a density of 5000 cells/well, they were left 24 h to allow the adherence of the cells. After that, the cells were stimulated with the IC_{50} of the extract fraction of *A. lechuguilla*, DMSO (0.1%) was used as a negative control and Paclitaxel (5.0 µg/mL) as positive control. The assays were carried out at 6, 12 and 24 h, after that time the cells were trypsinized and collected in cytometry tubes, centrifuged at 1400 RPM for 5 min, and the supernatant was discarded.

The cells were resuspended in 500 µL of binding buffer (1×), 1 µL of Annexin V-APC and 1 µL of 7-AAD were added and the samples were incubated for 15 min in the dark. Finally, samples were read

on an Accuri flow cytometer (Becton Dickinson, San Diego, CA, USA), and analyzed with the FlowJo software (v10.4.2 LLC, Ahsland, OR, USA).

3.8. In Silico Analysis

To explore the structural mechanism by which these molecules present in the fractionated hydrolyzed extract of *lechuguilla*, an *in silico* analysis through molecular docking was performed. Computational dockings calculations were carried out by using the DockingServer [53]. Employing Fas/CD95 [2NA7], TNF-R1 [2ZJC], DR4 [5CIR], DR5 [1D0G], tBID [2M5I], Bax [2G5B], Bak [2JCN], BCl-2 [5FCG], Casp-3 [1NME], Casp-8 [3KJQ], RIP1 [4ITJ], FADD [1E3Y], MLKL [4M67], ALK [2YHV], EGFR [1IVO], K-Ras [3GFT], TGFBR [3KED], MEK [3MBL], and MAPK [3TG3] the codes in square bracket refer to protein data bank entries (protein crystal structures). Molecules were downloaded from PubChem and the docetaxel and dimer of flavonoid were designed by using ChemProfessional 15.0 (v15.0.0.106 Chemdraw, PerkinElmer Informatics, MA, USA). Gaesteiger partial charges were added to the ligand atoms. Non-polar hydrogens atoms were merged, and rotatable bonds were defined. The MMFF94 force field was used for the energy minimization of ligand molecules. Docking simulations were performed by using the LGA. Each docking experiment was derived from 100 different runs that were set to terminate after a maximum of 2,500,000 energy evaluations. The population size was set up to 150. During the search, a translational step of 0.2 Å, and quaternion and torsion steps of 5 were applied.

4. Conclusions

The biflavonoid found by mass spectrometry, together with the flavonoids kaempferol and quercetin, turned out to be a mixture with synergistic activity on the cell viability of SK-LU-1, considering the IC_{50}, the induction of apoptosis and the possible activation of the signaling pathways both extrinsic and intrinsic, and blocking signaling on the EGFR and K-Ras, were studied through molecular docking. The reduction of cell viability is not related to the antioxidant capacity, it rather depends on the specific interaction of the ligands with the membrane receptors of the signaling pathways of the induction of apoptosis. Molecular docking enabled us to demonstrate that the variety of molecules allows the generation of interactions with death receptors that provoke apoptosis by the extrinsic pathway; as well as through the intrinsic pathway by tBID, as generator of the cytochrome C formation, and consequently, the activation of caspase-3, amplifying the apoptotic signal, in addition to showing possible inhibition in EGFR and K-Ras by stopping the growth of lung cancer cells. In general, the mixture of the three flavonoids (kaempferol, quercetin y biflavonoid) can be used as therapeutic targets, due to the activation of death receptors and caspases-3 and -8.

It is necessary to carry out studies on the interaction of the ligands, receptors and proteins involved in the signaling pathways, along with to evaluating the response of the extract on carcinogenic lines that present the K-Ras mutation as: colon, pancreas or thyroid, as well as the effect of the extract enriched in flavonoids in vivo.

Supplementary Materials: Supplementary materials can be found at http://www.mdpi.com/1422-0067/19/12/3765/s1.

Author Contributions: M.E.J.-F. and E.L.-C. conceived and supervised the project performed the experimental methodology; L.A.A.-S. and M.E.J.-F. carried out the analysis, mass spectra and molecular dockings interpretation of the results; C.O.-P. supported the cells analysis, and interpretation of the cells results; J.L.R.-T. supervised the molecular dockings results. All authors reviewed the paper.

Funding: This research was funded by SIP-2018048; CONACYT-CB-2013-01 No. 220732-I010/532/2014.

Acknowledgments: L A.A.-S. is grateful for the Ph. D. scholarship (389231) from CONACYT.

Conflicts of Interest: The authors declare no conflict of interest.

Abbreviations

7-AAD	7-amino-actinomycin D
ACN	Acetonitrile
ALK	Anaplastic lymphoma kinase
APC	Aloficocianina
BID	BH3 interacting-domain death agonist
Caspases	Cysteine aspartate-specific proteases
CML	Chronic myelogenous leukemia
DISC	Death inducing signaling complex
DMSO	Dimethyl sulfoxide
DR	Death receptor
EDTA	2,2′,2″,2‴-(Ethane-1,2-diyldinitrilo) tetraacetic acid
EGFR	Epidermal growth factor receptor
FADD	Fas-associated death domain protein
FBS	Fetal bovine serum
FITC	Fluorescein
IC	Inhibitory concentration
K-Ras	Kirsten rat sarcoma virus
LGA	Lamarckian genetic algorithm
MAPK	Mitogen activated protein kinase
MEK	MARK/ERK kinase
MLKL	Mixed lineage kinase domain like protein
MTT	3-(4,5-diMethyl-2-Thiazolyl)-2,5-diphenyl-2H-Tetrazolium bromide
NSCLC	Not-small cell lung cancer
OD	Optical density
ORAC	Oxygen radical absorbance capacity
PBS	Phosphate buffered saline
PM	Particulate matter
RIP	Receptor-interacting protein
RPM	Revolutions per minute
SCLC	Small cell lung cancer
SRB	Sulforhodamine B
tBID	Truncated BID
TGFβ receptor	Transforming growth factor beta receptor
TEAC	Trolox equivalent antioxidant capacity
TCA	Trichloroacetic acid
TFA	Trifluoroacetic acid
TNF	Tumor necrosis factor
Tris	Tris(hydroxymethyl)aminomethane
UNAM	Universidad Nacional Autónoma de México

References

1. Zhang, Y.-J.; Gan, R.-Y.; Li, S.; Zhou, Y.; Li, A.-N.; Xu, D.-P.; Li, H.-B.; Zhang, Y.-J.; Gan, R.-Y.; Li, S.; et al. Antioxidant Phytochemicals for the Prevention and Treatment of Chronic Diseases. *Molecules* **2015**, *20*, 21138–21156. [CrossRef] [PubMed]
2. Global Cancer Observatory. Available online: http://gco.iarc.fr/ (accessed on 26 September 2018).
3. Downward, J. Targeting RAS signalling pathways in cancer therapy. *Nat. Rev. Cancer* **2003**, *3*, 11–22. [CrossRef] [PubMed]
4. Gazdar, A.F.; Girard, L.; Lockwood, W.W.; Lam, W.L.; Minna, J.D. Lung cancer cell lines as tools for biomedical discovery and research. *J. Natl. Cancer Inst.* **2010**, *102*, 1310–1321. [CrossRef] [PubMed]
5. Sun, S.; Schiller, J.H.; Gazdar, A.F. Lung cancer in never smokers—A different disease. *Nat. Rev. Cancer* **2007**, *7*, 778–790. [CrossRef] [PubMed]

6. Lee, W.-H.; Loo, C.-Y.; Ghadiri, M.; Leong, C.-R.; Young, P.M.; Traini, D. The potential to treat lung cancer via inhalation of repurposed drugs. *Adv. Drug Deliv. Rev.* **2018**. [CrossRef] [PubMed]
7. Karapetis, C.S.; Khambata-Ford, S.; Jonker, D.J.; O'Callaghan, C.J.; Tu, D.; Tebbutt, N.C.; Simes, R.J.; Chalchal, H.; Shapiro, J.D.; Robitaille, S.; et al. K-ras Mutations and Benefit from Cetuximab in Advanced Colorectal Cancer. *N. Engl. J. Med.* **2008**, *359*, 1757–1765. [CrossRef] [PubMed]
8. Lissowska, J.; Foretova, L.; Dąbek, J.; Zaridze, D.; Szeszenia-Dabrowska, N.; Rudnai, P.; Fabianova, E.; Cassidy, A.; Mates, D.; Bencko, V.; et al. Family history and lung cancer risk: International multicentre case–control study in Eastern and Central Europe and meta-analyses. *Cancer Causes Control* **2010**, *21*, 1091–1104. [CrossRef] [PubMed]
9. Greiser, C.M.; Greiser, E.M.; Dören, M. Menopausal hormone therapy and risk of lung cancer—Systematic review and meta-analysis. *Maturitas* **2010**, *65*, 198–204. [CrossRef] [PubMed]
10. Hackshaw, A.K.; Law, M.R.; Wald, N.J. The accumulated evidence on lung cancer and environmental tobacco smoke. *BMJ* **1997**, *315*, 980–988. [CrossRef] [PubMed]
11. Lim, C.C.; Hayes, R.B.; Ahn, J.; Shao, Y.; Silverman, D.T.; Jones, R.R.; Garcia, C.; Thurston, G.D. Association between long-term exposure to ambient air pollution and diabetes mortality in the US. *Environ. Res.* **2018**, *165*, 330–336. [CrossRef] [PubMed]
12. Zhao, Y.; Wang, S.; Aunan, K.; Martin Seip, H.; Hao, J. Air pollution and lung cancer risks in China—A meta-analysis. *Sci. Total Environ.* **2006**, *366*, 500–513. [CrossRef] [PubMed]
13. Lissowska, J.; Bardin-Mikolajczak, A.; Fletcher, T.; Zaridze, D.; Szeszenia-Dabrowska, N.; Rudnai, P.; Fabianova, E.; Cassidy, A.; Mates, D.; Holcatova, I.; et al. Lung Cancer and Indoor Pollution from Heating and Cooking with Solid FuelsThe IARC International Multicentre Case-Control Study in Eastern/Central Europe and the United Kingdom. *Am. J. Epidemiol.* **2005**, *162*, 326–333. [CrossRef] [PubMed]
14. Brenner, D.R.; McLaughlin, J.R.; Hung, R.J. Previous Lung Diseases and Lung Cancer Risk: A Systematic Review and Meta-Analysis. *PLoS ONE* **2011**, *6*, e17479. [CrossRef] [PubMed]
15. Miller, A.B.; Altenburg, H.-P.; Bueno-de-Mesquita, B.; Boshuizen, H.C.; Agudo, A.; Berrino, F.; Gram, I.T.; Janson, L.; Linseisen, J.; Overvad, K.; et al. Fruits and vegetables and lung cancer: Findings from the European Prospective Investigation into Cancer and Nutrition. *Int. J. Cancer* **2004**, *108*, 269–276. [CrossRef] [PubMed]
16. Heim, K.E.; Tagliaferro, A.R.; Bobilya, D.J. Flavonoid antioxidants: Chemistry, metabolism and structure-activity relationships. *J. Nutr. Biochem.* **2002**, *13*, 572–584. [CrossRef]
17. Sidana, J.; Singh, B.; Sharma, O.P. Saponins of Agave: Chemistry and bioactivity. *Phytochemistry* **2016**, *130*, 22–46. [CrossRef] [PubMed]
18. Yang, C.-R.; Zhang, Y.; Jacob, M.R.; Khan, S.I.; Zhang, Y.-J.; Li, X.-C. Antifungal Activity of C-27 Steroidal Saponins. *Antimicrob. Agents Chemother.* **2006**, *50*, 1710–1714. [CrossRef] [PubMed]
19. Santos, J.; Vieira, I.; Braz-Filho, R.; Branco, A.; Santos, J.D.G.; Vieira, I.J.C.; Braz-Filho, R.; Branco, A. Chemicals from Agave sisalana Biomass: Isolation and Identification. *Int. J. Mol. Sci.* **2015**, *16*, 8761–8771. [CrossRef] [PubMed]
20. Rizwan, K.; Zubair, M.; Rasool, N.; Riaz, M.; Zia-Ul-Haq, M.; de Feo, V.; Rizwan, K.; Zubair, M.; Rasool, N.; Riaz, M.; et al. Phytochemical and Biological Studies of Agave attenuata. *Int. J. Mol. Sci.* **2012**, *13*, 6440–6451. [CrossRef] [PubMed]
21. Carmona, J.E.; Morales-Martínez, T.K.; Mussatto, S.I.; Castillo-Quiroz, D.; Ríos-González, L.J. Propiedades químicas, estructurales y funcionales de la lechuguilla (Agave lechuguilla Torr.). *Rev. Mex. Cienc. For.* **2017**, *8*, 100–122.
22. Blando-Navarrete, J.L.; Baca-Marin, S. Determinación del potencial productivo de la lechuguilla (Agave lechuguilla Torr) en el municipio de San Juan de Guadalupe Dgo. *Rev. Chapingo Ser. Zonas Áridas* **2001**, *II*, 100–105.
23. Reyes-Agüero, J.A.; Aguirre-Rivera, J.R.; Peña-Valdivía, C.B. Biología y aprovechamiento de Agave lechuguilla Torrey. *Bol. Soc. Botánica México* **2000**, *67*, 75–88.
24. Nava-Cruz, N.Y.; Medina-Morales, M.A.; Martinez, J.L.; Rodriguez, R.; Aguilar, C.N. Agave biotechnology: An overview. *Crit. Rev. Biotechnol.* **2015**, *35*, 546–559. [CrossRef] [PubMed]
25. March, R.E.; Miao, X.-S. A fragmentation study of kaempferol using electrospray quadrupole time-of-flight mass spectrometry at high mass resolution. *Spec. Issue Honour Jean-Claude Tabet* **2004**, *231*, 157–167. [CrossRef]

26. Justino, G.C.; Borges, C.M.; Florêncio, M.H. Electrospray ionization tandem mass spectrometry fragmentation of protonated flavone and flavonol aglycones: A re-examination. *Rapid Commun. Mass Spectrom.* **2009**, *23*, 237–248. [CrossRef] [PubMed]
27. Florita Ramos Casillas, Cytotoxic activity of Agave lechuguilla Torr. *Afr. J. Biotechnol.* **2012**, *11*. [CrossRef]
28. Sak, K. Cytotoxicity of dietary flavonoids on different human cancer types. *Pharmacogn. Rev.* **2014**, *8*, 122–146. [CrossRef] [PubMed]
29. Bikadi, Z.; Hazai, E. Application of the PM6 semi-empirical method to modeling proteins enhances docking accuracy of AutoDock. *J. Cheminform.* **2009**, *1*, 15. [CrossRef] [PubMed]
30. L Rosas-Trigueros, J.; Ilizaliturri-Flores, I.; G Benitez-Cardoza, C.; Correa-Basurto, J.; Zamorano-Carrillo, A. Computational Modeling and Simulation of the Bcl-2 Family: Paving the Way for Rational Drug Design. *Curr. Med. Chem.* **2012**, *19*, 6081–6094. [CrossRef]
31. Li, J.; Yin, Q.; Wu, H. Chapter Five—Structural Basis of Signal Transduction in the TNF Receptor Superfamily. In *Advances in Immunology*; Alt, F.W., Ed.; Academic Press: Cambridge, MA, USA, 2013; Volume 119, pp. 135–153, ISBN 0065-2776.
32. Kantari, C.; Walczak, H. Caspase-8 and Bid: Caught in the act between death receptors and mitochondria. *Mitochondria Deadly Organelle* **2011**, *1813*, 558–563. [CrossRef] [PubMed]
33. Spetz, J.; Presser, A.G.; Sarosiek, K.A. T Cells and Regulated Cell Death: Kill or Be Killed. In *International Review of Cell and Molecular Biology*; Academic Press: Cambridge, MA, USA, 2018; ISBN 1937-6448.
34. Sathishkumar, N.; Sathiyamoorthy, S.; Ramya, M.; Yang, D.-U.; Lee, H.N.; Yang, D.-C. Molecular docking studies of anti-apoptotic BCL-2, BCL-XL, and MCL-1 proteins with ginsenosides from Panax ginseng. *J. Enzyme Inhib. Med. Chem.* **2012**, *27*, 685–692. [CrossRef] [PubMed]
35. Li, J.; McQuade, T.; Siemer, A.B.; Napetschnig, J.; Moriwaki, K.; Hsiao, Y.-S.; Damko, E.; Moquin, D.; Walz, T.; McDermott, A.; et al. The RIP1/RIP3 Necrosome Forms a Functional Amyloid Signaling Complex Required for Programmed Necrosis. *Cell* **2012**, *150*, 339–350. [CrossRef] [PubMed]
36. Román, M.; Baraibar, I.; López, I.; Nadal, E.; Rolfo, C.; Vicent, S.; Gil-Bazo, I. KRAS oncogene in non-small cell lung cancer: Clinical perspectives on the treatment of an old target. *Mol. Cancer* **2018**, *17*, 33. [CrossRef] [PubMed]
37. Vander Ark, A.; Cao, J.; Li, X. TGF-β receptors: In and beyond TGF-β signaling. *Cell. Signal.* **2018**, *52*, 112–120. [CrossRef] [PubMed]
38. Cole, S.P.C. Multidrug resistance protein 1 (MRP1, ABCC1), a "multitasking" ATP-binding cassette (ABC) transporter. *J. Biol. Chem.* **2014**, *289*, 30880–30888. [CrossRef] [PubMed]
39. Troy, A. Baudino Targeted Cancer Therapy: The Next Generation of Cancer Treatment. *Curr. Drug Discov. Technol.* **2015**, *12*, 3–20. [CrossRef]
40. Li, Y.H.; Yu, C.Y.; Li, X.X.; Zhang, P.; Tang, J.; Yang, Q.; Fu, T.; Zhang, X.; Cui, X.; Tu, G.; et al. Therapeutic target database update 2018: Enriched resource for facilitating bench-to-clinic research of targeted therapeutics. *Nucleic Acids Res.* **2018**, *46*, D1121–D1127. [CrossRef] [PubMed]
41. Pluchino, K.M.; Hall, M.D.; Goldsborough, A.S.; Callaghan, R.; Gottesman, M.M. Collateral sensitivity as a strategy against cancer multidrug resistance. *Drug Resist. Updat.* **2012**, *15*, 98–105. [CrossRef] [PubMed]
42. Vicente-Vicente, L.; Prieto, M.; Morales, A.I. Eficacia y seguridad de la quercetina como complemento alimenticio. *Rev. Toxicol.* **2013**, *30*, 171–181.
43. Dunnick, J.K.; Hailey, J.R. Toxicity and carcinogenicity studies of quercetin, a natural component of foods. *Fundam. Appl. Toxicol. Off. J. Soc. Toxicol.* **1992**, *19*, 423–431.
44. Haghi, G.; Hatami, A. Simultaneous quantification of flavonoids and phenolic acids in plant materials by a newly developed isocratic high-performance liquid chromatography approach. *J. Agric. Food Chem.* **2010**, *58*, 10812–10816. [CrossRef] [PubMed]
45. Vázquez, C.V.; Rojas, M.G.V.; Ramírez, C.A.; Chávez-Servín, J.L.; García-Gasca, T.; Ferriz Martínez, R.A.; García, O.P.; Rosado, J.L.; López-Sabater, C.M.; Castellote, A.I.; et al. Total phenolic compounds in milk from different species. Design of an extraction technique for quantification using the Folin–Ciocalteu method. *Food Chem.* **2015**, *176*, 480–486. [CrossRef] [PubMed]
46. Herald, T.J.; Gadgil, P.; Tilley, M. High-throughput micro plate assays for screening flavonoid content and DPPH-scavenging activity in sorghum bran and flour. *J. Sci. Food Agric.* **2012**, *92*, 2326–2331. [CrossRef] [PubMed]

47. Kambayashi, Y.; Binh, N.T.; Asakura, H.W.; Hibino, Y.; Hitomi, Y.; Nakamura, H.; Ogino, K. Efficient Assay for Total Antioxidant Capacity in Human Plasma Using a 96-Well Microplate. *J. Clin. Biochem. Nutr.* **2009**, *44*, 46–51. [CrossRef] [PubMed]
48. Alvarez-Parrilla, E.; de la Rosa, L.A.; Amarowicz, R.; Shahidi, F. Antioxidant Activity of Fresh and Processed Jalapeño and Serrano Peppers. *J. Agric. Food Chem.* **2011**, *59*, 163–173. [CrossRef] [PubMed]
49. Abel, S.D.A.; Baird, S.K. Honey is cytotoxic towards prostate cancer cells but interacts with the MTT reagent: Considerations for the choice of cell viability assay. *Food Chem.* **2018**, *241*, 70–78. [CrossRef] [PubMed]
50. Kurtz, S.L.; Lawson, L.B. Determination of permeation pathways of hydrophilic or hydrophobic dyes through the mammary papilla. *Int. J. Pharm.* **2018**, *545*, 10–18. [CrossRef] [PubMed]
51. Eisenbrand, G.; Pool-Zobel, B.; Baker, V.; Balls, M.; Blaauboer, B.; Boobis, A.; Carere, A.; Kevekordes, S.; Lhuguenot, J.-C.; Pieters, R.; et al. Methods of in vitro toxicology. *Food Chem. Toxicol.* **2002**, *40*, 193–236. [CrossRef]
52. Mosmann, T. Rapid colorimetric assay for cellular growth and survival: Application to proliferation and cytotoxicity assays. *J. Immunol. Methods* **1983**, *65*, 55–63. [CrossRef]
53. Virtua Drug Ltd. Molecular Docking Server. Available online: https://www.dockingserver.com/web (accessed on 5 September 2018).